Addendum to the MiniBooNE Run Plan: Run Request for an Anti-Neutrino Oscillation Analysis

October 1, 2007

A. A. Aguilar-Arevalo[4], C. Anderson[15], S. J. Brice[5], B. C. Brown[5], L. Bugel[4], L. Coney[7], J. M. Conrad[4], D. C. Cox[9], Z. Djurcic[4], D. A. Finley[5], B. T. Fleming[15], R. Ford[5], F. G. Garcia[5], G. T. Garvey[10], C. Green[5,10], J. A. Green[9,10], E. Hawker[8], R. Imlay[11], R. A. Johnson[2], G. Karagiorgi[4], P. Kasper[5], T. Katori[9], T. Kobilarcik[5], I. Kourbanis[5], S. Linden[15], J. M. Link[14], Y. Liu[1], W. C. Louis[10], K. B. M. Mahn[4], C. Mariani[4], W. Marsh[5], W. Metcalf[11], G. B. Mills[10], C. D. Moore[5], R. H. Nelson[3], V. Nguyen[4], P. Nienaber[13], S. Ouedraogo[11], D. Perevalov[1], C. C. Polly[9], E. Prebys[5], H. Ray[6], B. P. Roe[12], A. D. Russell[5], D. Schmitz[4], M. H. Shaevitz[4], M. Soderberg[15], M. Sorel[4], P. Spentzouris[5], J. Spitz[15], I. Stancu[1], R. J. Stefanski[5], R. Tayloe[9], M. Tzanov[3], R. Van de Water[10], M. O. Wascko[11], D. H. White[10], M. J. Wilking[3], H. J. Yang[12], G. P. Zeller[10], E. D. Zimmerman[3]

(The MiniBooNE Collaboration)

[1] *University of Alabama; Tuscaloosa, AL 35487*
[2] *University of Cincinnati; Cincinnati, OH 45221*
[3] *University of Colorado; Boulder, CO 80309*
[4] *Columbia University; New York, NY 10027*
[5] *Fermi National Accelerator Laboratory; Batavia, IL 60510*
[6] *University of Florida; Gainesville, FL 32611*
[7] *Hope College; Holland, MI 49423*
[8] *Illinois Mathematics and Science Academy; Aurora, IL 60506*
[9] *Indiana University; Bloomington, IN 47405*
[10] *Los Alamos National Laboratory; Los Alamos, NM 87545*
[11] *Louisiana State University; Baton Rouge, LA 70803*
[12] *University of Michigan; Ann Arbor, MI 48109*
[13] *Saint Mary's University of Minnesota; Winona, MN 55987*
[14] *Virginia Polytechnic Institute & State University; Blacksburg, VA 24061*
[15] *Yale University; New Haven, CT 06520*

Contents

1 Executive Summary

MiniBooNE has accumulated 5.58×10^{20} protons on target (POT) with the horn in neutrino mode and, earlier this year, published a search for ν_e appearance that ruled out a two neutrino oscillation interpretation of the results of the LSND experiment [23]. These data also showed an excess of ν_e candidates at low energy that is under active investigation and the wider data set is being used to make a suite of neutrino cross-section measurements. At this time the collaboration believes there is no compelling need for more neutrino mode data.

Since January of 2006 the beamline has run with the horn in anti-neutrino mode and has so far accumulated 2.33×10^{20} POT in that configuration. As laid out in the documents that requested this running period [26, 27], these events are being used to make a series of anti-neutrino cross-section measurements and a search for anti-numu disappearance. The 2.33×10^{20} POT are still considered sufficient to make these measurements. There is one crucial analysis, however, that would significantly benefit from more POT: a search for $\bar{\nu}_e$ appearance. The LSND result was an indication of *anti-*ν_e appearance and hence it is critical that MiniBooNE test LSND in anti-neutrino mode as well as with the already published neutrino mode search.

With 2.33×10^{20} POT in anti-neutrino mode MiniBooNE is insensitive to much of the LSND allowed parameter space, but if these data were increased to 5.0×10^{20} POT then the coverage of the LSND region would be significantly improved. In FY2008 the Booster Neutrino Beamline (BNB) is slated to provide 1.0×10^{20} POT in neutrino mode and 1.0×10^{20} POT in anti-neutrino mode; this is the already approved SciBooNE run. Having the BNB deliver 2.0×10^{20} POT in FY2009 is within the projections of the Proton Source Department. MiniBooNE therefore makes the following request:

> *MiniBooNE requests an additional* 3.0×10^{20} *POT in anti-neutrino mode to give the experiment a total of* 5.0×10^{20} *POT in this configuration and enable a powerful check of the LSND result in anti-neutrinos. The experiment further requests that these POT be delivered in FY2008 and FY2009.*

2 Introduction

MiniBooNE was motivated by the result from the Liquid Scintillator Neutrino Detector (LSND) experiment [1] in the mid 1990's, which presented evidence for $\bar{\nu}_\mu \rightarrow \bar{\nu}_e$ oscillations at the $\Delta m^2 \sim 1$ eV^2 scale. The 3.8σ excess of electron anti-neutrino candidates seen by LSND would correspond to a $\bar{\nu}_\mu \rightarrow \bar{\nu}_e$ oscillation probability of $0.26 \pm 0.08\%$. While the KARMEN experiment observed no evidence for neutrino oscillations [2], a joint analysis [3] showed compatibility at the 64% C.L. Solar neutrino [4, 5, 6, 8, 7], atmospheric neutrino [9, 10, 11, 12], long-baseline accelerator neutrino [13, 14] and reactor anti-neutrino experiments [15] have convincing evidence for neutrino oscillations, but at two Δm^2 scales very different from that indicated by the LSND result. This would necessitate the introduction of one or more new neutrino states (which must be sterile [16]) or other extensions to the Standard Model.

MiniBooNE was built with a baseline and a neutrino energy spectrum peak both roughly ten times that of LSND. This enables the experiment to be sensitive to roughly the same oscillation phase space, since L/E was the same as that of LSND, but with very different systematics, as the neutrino energy is so much higher.

Between 2002 and late 2005 MiniBooNE accumulated 5.58×10^{20} protons on target in neutrino mode (the configuration where the horn focuses positively charged particles). With these data, the experiment searched for evidence of electron neutrino appearance consistent with an oscillation interpretation of LSND. The analysis, done via two independent methods, was released in April 2007 [23] and ruled out a two-neutrino oscillation interpretation of LSND by looking above a neutrino energy threshold of 475 MeV. The neutrino energy histogram of electron neutrino candidates and the curves showing the excluded region of oscillation space are shown in Figs. 1 and 2. Below 475 MeV neutrino energy there is an excess of events in the data. This area is currently under intense study.

The sources of systematic error in the measurement divide into three categories: uncertainties in the neutrino fluxes, uncertainties in the neutrino cross sections, and uncertainties in the modeling of the detector. These groups of errors are taken to be independent, and an individual error matrix is formed for each that includes the full correlation among the systematic parameters. This is mapped to a matrix describing the correlated errors in predicted background plus possible signal in eight ν_e E_ν^{QE} bins. The final covariance matrix for all sources of uncertainty (statistical and systematic) is the sum of the individual error matrices. This method of estimation of systematic uncertainties is CPU intensive, but, once set up, can be used to estimate errors for any MiniBooNE dataset. In particular this system has been used in this document to produce a complete estimate of the uncertainties associated with a $\bar{\nu}_e$ sample used to search for $\bar{\nu}_e$ appearance oscillations. The signal extraction is performed by computing the χ^2 comparing data to predicted background plus a $(\sin^2(2\theta), \Delta m^2)$-determined contribution from $\nu_\mu \rightarrow \nu_e$ two-neutrino oscillations in the eight E_ν^{QE} bins; this quantity is then minimized with respect to these two oscillation parameters across their physical range. When setting limits or calculating sensitivity curves a raster scan in Δm^2 is performed and for each raster a single parameter, one sided confidence point is found. The set of these points forms the limit/sensitivity curve.

With the 5.58×10^{20} POT in neutrino mode MiniBooNE is also pursuing a number

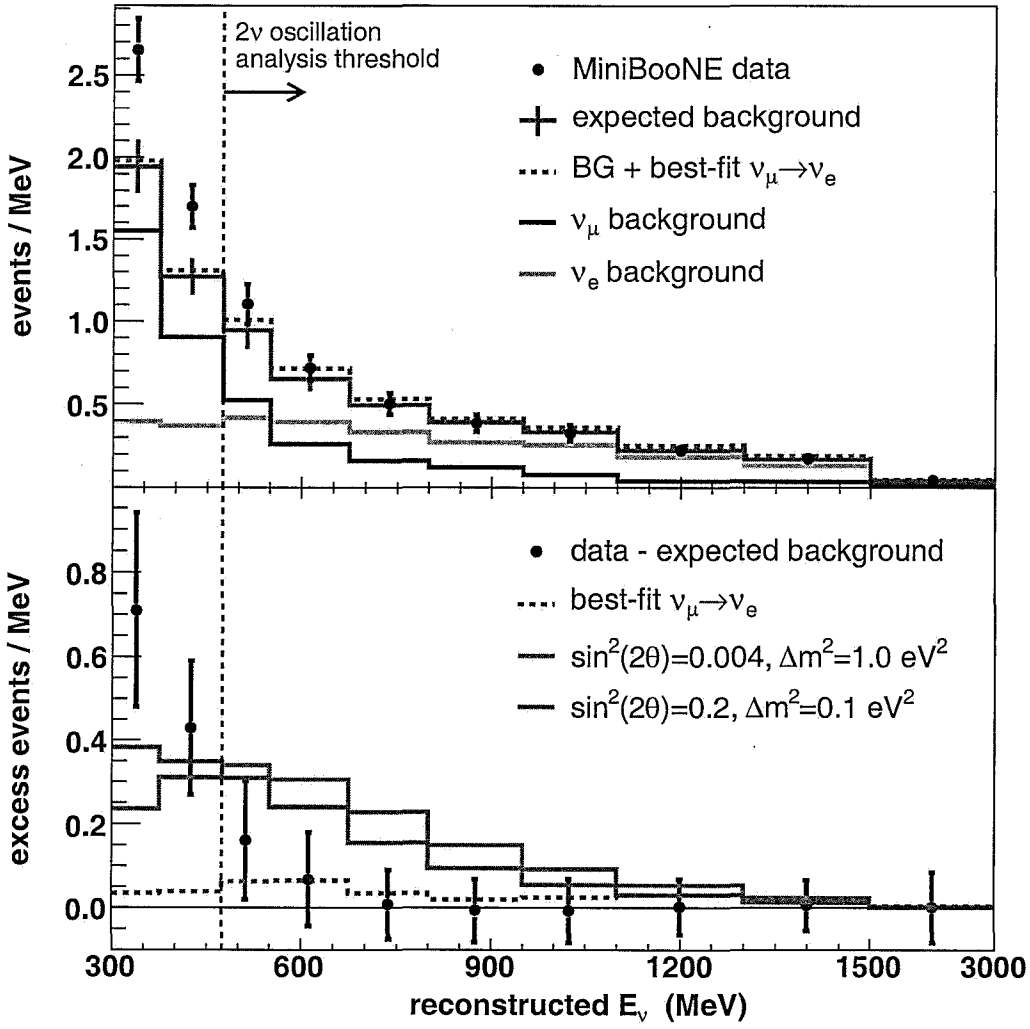

Figure 1: *The top plot shows the number of candidate ν_e events as a function of E_ν^{QE}. The points represent the data with statistical error, while the histogram is the expected background with systematic errors from all sources. The vertical dashed line indicates the threshold used in the two-neutrino oscillation analysis. Also shown are the best-fit oscillation spectrum (dashed histogram) and the background contributions from ν_μ and ν_e events. The bottom plot shows the number of events with the predicted background subtracted as a function of E_ν^{QE}, where the points represent the data with total errors and the two histograms correspond to LSND solutions at high and low Δm^2.*

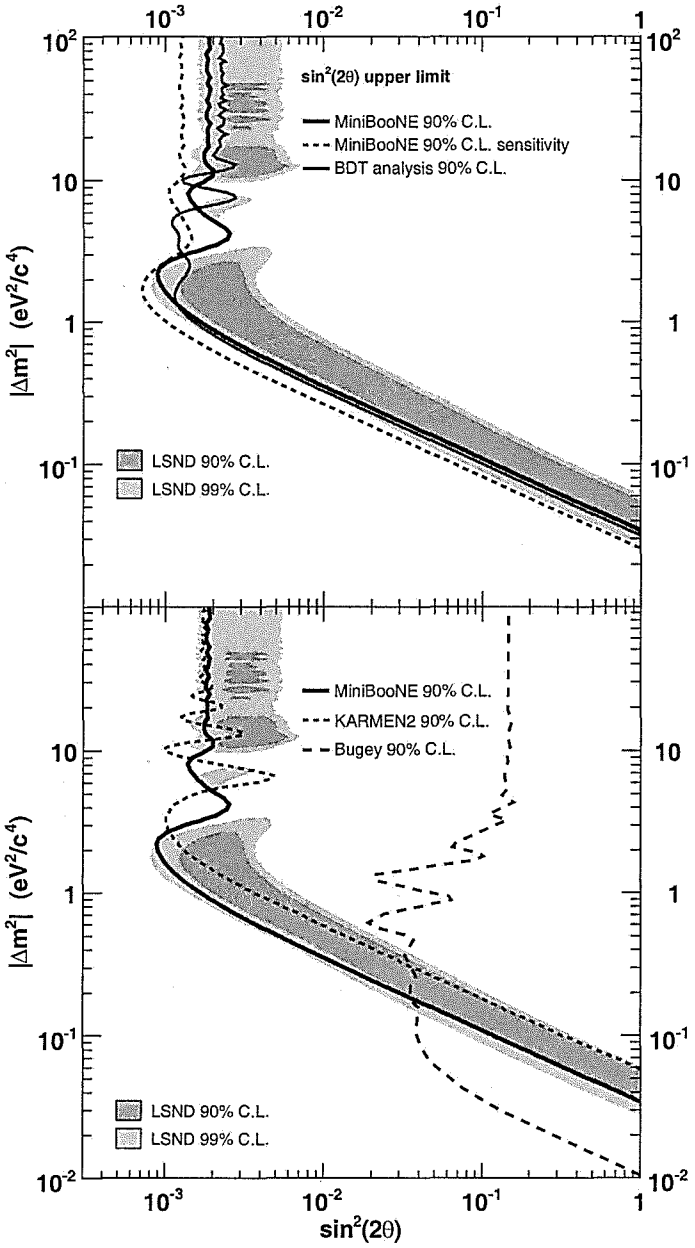

Figure 2: *The top plot shows the MiniBooNE 90% CL limit (thick solid curve) and sensitivity (dashed curve) for events with* $475 < E_\nu^{QE} < 3000$ *MeV within a two-neutrino oscillation model. Also shown is the limit from the boosted decision tree analysis (thin solid curve) for events with* $300 < E_\nu^{QE} < 3000$ *MeV. The bottom plot shows the limits from the KARMEN [2] and Bugey [22] experiments. The MiniBooNE and Bugey curves are one-sided upper limits on* $\sin^2 2\theta$ *corresponding to* $\Delta\chi^2 = 1.64$*, while the KARMEN curve is a "unified approach" 2D contour. The shaded areas show the 90% and 99% CL allowed regions from the LSND experiment.*

of other analyzes each of which have, or will shortly, yield publications. At the start of 2006 MiniBooNE switched to running in anti-neutrino mode (where the horn focuses negatively charged particles) and since that time has accumulated 2.33×10^{20} POT in that configuration. As described in previous submissions to the PAC [26, 27], a suite of measurements are also being pursued using this dataset.

3 Anti-Neutrino Sensitivity

In previous requests to the PAC, MiniBooNE has asked for running in anti-neutrino mode to make a set of ground-breaking anti-neutrino cross-section measurements and to make a search for $\bar{\nu}_\mu$ disappearance. Notably absent from these requests was the possibility of using the requested POT to make a search for $\bar{\nu}_e$ appearance oscillations. Since anti-neutrino charged current cross-sections are typically a factor of ~ 3 less than their neutrino equivalents, and since the flux in anti-neutrino mode is almost a factor of 2 smaller than in neutrino mode, it was known in each of the previous requests that a $\bar{\nu}_e$ appearance measurement would need more POT than were being asked for at the time. The present request, however, is for enough additional anti-neutrino mode POT to perform a $\bar{\nu}_e$ appearance search.

MiniBooNE has now completed the ν_e appearance analysis and with it a complete assessment of all the relevant systematics. As explained in Sec. 2, the systematic uncertainties were determined by assessing all the low level uncertainties in processes such as pion production in p-Be collisions and the uncertain parameters of neutrino cross-sections, and then propagating these uncertainties into an error matrix in the final neutrino energy histogram. This method can be readily transferred to the $\bar{\nu}_e$ appearance analysis; this section shows the results of that transfer.

In the ν_e appearance result the systematic errors were larger that the statistical, though not dominantly so. This gives reason to hope that despite the lower interaction rate (a factor of ~ 5 for the same POT), a $\bar{\nu}_e$ appearance search might have "similar" sensitivity to the ν_e appearance result for a comparable number of protons on target. Fig. 3 shows the MiniBooNE $\bar{\nu}_e$ appearance sensitivity curves for 2.33×10^{20}, 5.0×10^{20}, and 10.0×10^{20} delivered POT. As Sec. 4 explains, the already delivered 2.33×10^{20} POT corresponds to 2.0×10^{20} POT in usuable statistics. These curves have been laid over the region allowed at 90% by a joint analysis of LSND and KARMEN [3].

For the total of 5.0×10^{20} POT in anti-neutrino mode requested in this document, Fig. 4 shows the sensitivity curves that result when one considers statistical errors only (red curve), statistical plus detector (optical model) errors (green curve), and all relevant errors except the contribution from dirt events (blue curve). The blue curve in Fig. 4 is identical to the cyan curve in Fig. 3. In Fig. 4 the curves are laid over the region allowed at 90% and 99% by LSND alone; this allows direct comparison with the neutrino mode exclusion limit result of Fig.2. In keeping with the neutrino mode oscillation analysis the sensitivities shown here only consider events with a reconstructed neutrino energy above 475 MeV. A couple of approximations have been made in the MiniBooNE curves of Figs. 3 and 4 for reasons of CPU time. The fractional effect of the detector optical model uncertainties on the $\bar{\nu}_e$ signal and background histograms has been taken from the neutrino mode error matrix rather

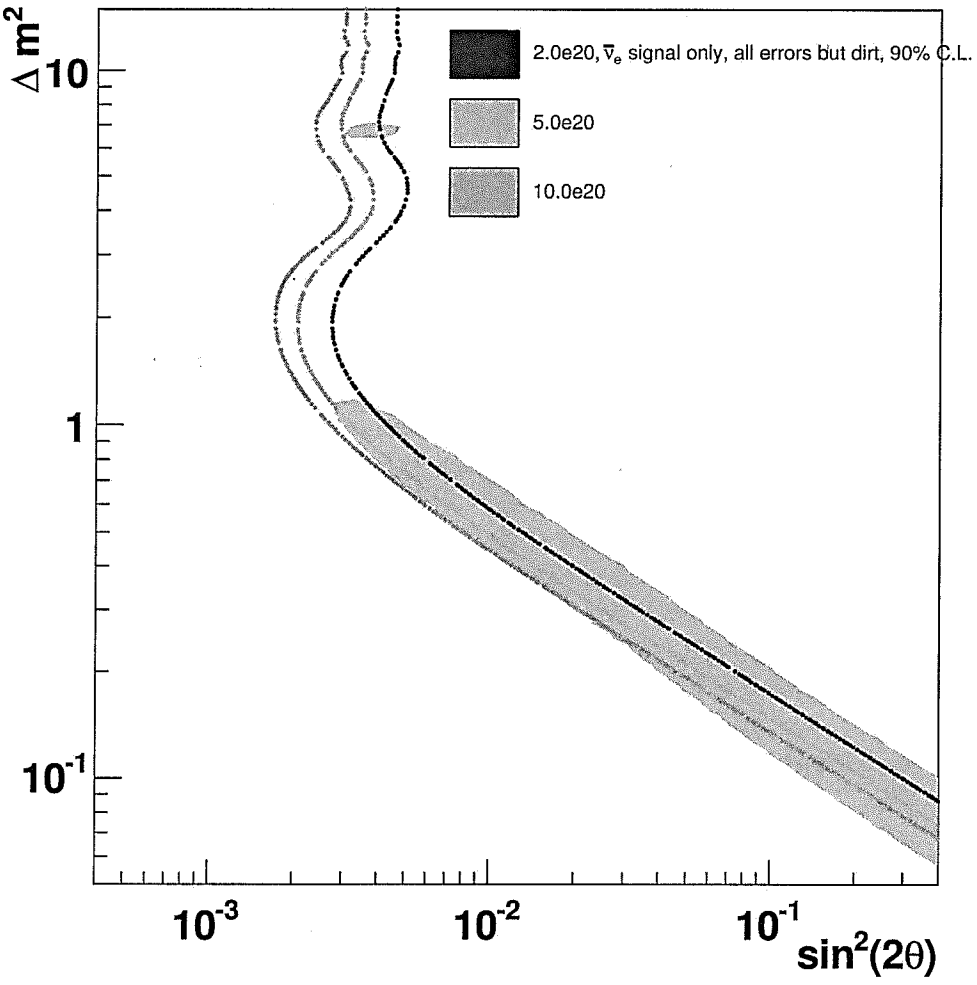

Figure 3: *The sensitivity to $\bar{\nu}_e$ oscillations for the already accumulated 2.33×10^{20} protons on target, for 5.0×10^{20}, and for 10.0×10^{20} POT. These curves are laid over the 90% confidence region that results from a combined fit to both LSND and KARMEN.*

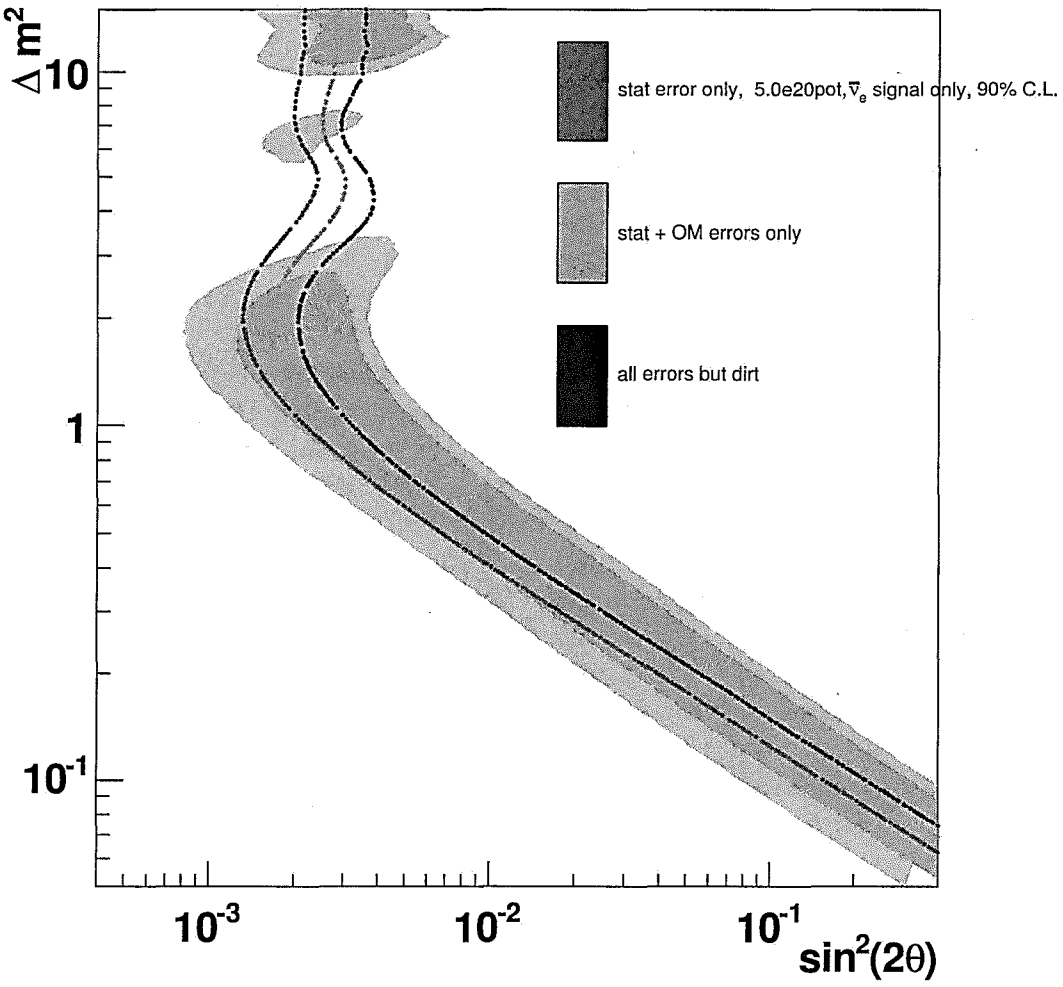

Figure 4: *The sensitivity to $\bar{\nu}_e$ oscillations for 5.0×10^{20} POT for statistical errors only (red), for statistical plus detector (optical model) errors (green), and for all relevant errors except the contribution from dirt events (blue). These curves are laid over the regions allowed at 90% and 99% C.L. by the LSND result. The sensitivity curves on this figure can be directly compared with the neutrino mode exclusion curves of Fig. 2.*

than being recalculated specifically for anti-neutrino mode, and the effect of backgrounds for neutrino interactions outside the tank have been left out. The optical model approximation is expected to be extremely good, but the absence of dirt backgrounds will make the curves of Figs. 3 and 4 slightly better than they should be. The effect will not change any conclusions drawn from these plots, but will result in future versions of these figures looking slightly different as the approximations are removed.

From Fig. 3 it is clear that 2.33×10^{20} delivered POT in anti-neutrino mode covers a sliver of the region allowed at 90% by a combined LSND-KARMEN analysis. However, the coverage is significantly expanded by increasing the dataset to 5.0×10^{20} POT. The 10.0×10^{20} POT curve is even better, of course, but it will be shown in Sec. 4 that this number of POT is probably not achievable within a reasonable time. The extra POT being requested will allow a real test of the LSND result in anti-neutrino mode.

4 Run Feasibility

The achievement of the physics goals outlined above depends critically on the experiment's ability to complete the run, i.e., can enough POT be accumulated in two years? Are there sufficient personnel to staff shifts and do the analysis? Is the apparatus sufficiently robust? and are there enough spare parts?

Table 1 shows the POT collected in the anti-neutrino run starting Jan 18, 2006. This corresponds to a total of 54 weeks of running. Due to hydrogen embrittlement of the chains suspending the 25 ton steel absorber plates, two separate plates fell into the decay pipe at different times. The biggest effect of this was to reduce the neutrino flux by 20% for one plate, and a total of 30% with two plates down. A further effect was a small distortion of the energy spectrum at low energy. However, a comparison of data and Monte Carlo shows that this distortion can be accurately reproduced and corrected in the analysis. Therefore, the data with the absorber plates are usable, with only a reduction in neutrino rates. Table 1 shows the POT corrected for this effect. The 2.33×10^{20} POT collected are equivalent to 2.03×10^{20} POT in anti-neutrinos with no absorber problem.

Condition	Total $\times 10^{20}$ POT	Corrected $\times 10^{20}$ POT
No absorber	1.15	1.15
One absorber plate down	0.57	0.45
Two absorber plates down	0.61	0.43
Totals	2.33	2.03

Table 1: *Integrated protons on target in anti-neutrino mode for various run conditions. The third column includes a correction for reduced neutrino rates due to the absorber.*

Proton delivery projections are generated as part of the "Proton Plan." In these estimates it is assumed that anti-proton production and the NuMI beamline have priority, and will get as many protons as the Main Injector can accelerate. It is

also assumed that the MiniBooNE experiment will get whatever protons the Proton Source can produce beyond that. Over the next year, both the protons to NuMI and the total Booster output are expected to increase, and because the MiniBooNE flux depends on the difference, this results in a significant uncertainty. This projection includes the negative effects of slip-stacking and positive effects of correctors and the improved running of the Booster achieved so far (the last three months of running prior to the 2007 shutdown achieved $\sim 0.5 \times 10^{19}$ POT/week, with NuMI running). In this scenario, the Booster should be able to continue delivering protons to MiniBooNE at roughly the $1 - 2 \times 10^{20}$ POT/year level for the next few years.

Running in FY2008 would be concurrent with SciBooNE. Their goal is to collect 1×10^{20} POT initially in neutrino mode, then switch to anti-neutrinos for a further 1×10^{20} POT. Thus, next year would only count as 1×10^{20} POT toward anti-neutrino data collected, and it would require a further year (2009) of anti-neutrino running to achieve the goal of an additional 3×10^{20} POT, to give a total of 5×10^{20} POT in anti-neutrinos.

The success of the run requires the personnel to staff shifts, and the reliability of the hardware and availability of spare parts for a further two years of operations. A three year projection of personnel available for running shifts, based on replies of collaboration members, is shown in Table 2. In FY2008 shift responsibilities would be shared with SciBooNE; beyond that MiniBooNE would be entirely responsible for shifts. As can be seen, there is 69% of shifters available in FY2009 compared to present. This can be offset by requiring more shifts per person, and allowing remote shift operations. A third year of running (FY2010) would see a 50% drop in shift personnel below present levels, making staffing shifts more problematic.

Year	Projected Shift personnel (FTE)
present	54
2008	44
2009	37
2010	29

Table 2: *Projected MiniBooNE shift personnel.*

With everything in place from the ν_e appearance result one can perform the $\bar{\nu}_e$ appearance analysis using these same tools. There will likely be some fresh optimizing of cuts and tuning of simulations, but nothing compared to the level of work required to produce the ν_e appearance result. Consequently, $\bar{\nu}_e$ appearance results are expected to be available shortly after the 5.0×10^{10} POT is accumulated.

The beamline, horn system, and detector have been operating well for the duration of the experiment since 2002. One horn replacement has been needed, and a repair of the 25 m absorber, but no major detector repairs or downtime have been incurred. A third horn and target are ready, as are spare accelerator parts, and spare detector electronics sufficient to run the experiment two more years. Also available is a fourth horn inner conductor (the part with the longest lead time). One possible trouble spot is the detector HVAC, which has been problematic over the years. It should continue to run for two more years with preventative maintenance and spare parts for the most

likely failure modes. An inspection of the 25 m absorber during the 2007 shutdown shows it to be working well with no corrosion present on the new hanging fixtures.

5 Summary

Increasing MiniBooNE's anti-neutrino POT from the current 2.33×10^{20} POT to 5.0×10^{20} POT will significantly increase the experiment's ability to test the LSND indication of oscillations. It should be remembered that the LSND measurement was an indication of *anti-*ν_e appearance and so it is imperative that MiniBooNE test it with anti-neutrinos as well as with the already published neutrino mode search. CP-violating models with the addition of two or more sterile neutrinos and which allow LSND style $\bar{\nu}_e$ appearance while showing no measurable ν_e appearance are allowed by all the existing data, albeit with some tension (see Appendix C).

The additional, requested POT should only take FY2008 and FY2009 running. This estimate allows for the approved SciBooNE running of 1.0×10^{20} POT in neutrino mode and 1.0×10^{20} POT in anti-neutrino mode in FY2008. To complete the picture Appendices A and B describe how the extra running might improve MiniBooNE's anti-neutrino cross-section measurements and whether it would shed any light on the excess of low energy electron neutrino candidates seen in neutrino mode.

References

[1] C. Athanassopoulos *et al.*, Phys. Rev. Lett. 75, 2650 (1995); C. Athanassopoulos *et al.*, Phys. Rev. Lett. 77, 3082 (1996); C. Athanassopoulos *et al.*, Phys. Rev. Lett. 81, 1774 (1998); A. Aguilar *et al.*, Phys. Rev. D 64, 112007 (2001).

[2] B. Armbruster *et al.*, Phys. Rev. D 65, 112001 (2002).

[3] E. Church *et al.*, Phys. Rev. D 66, 013001 (2002).

[4] B. T. Cleveland *et al.*, Astrophys. J. 496, 505 (1998).

[5] J. N. Abdurashitov *et al.*, Phys. Rev. C 60, 055801 (1999).

[6] W. Hampel *et al.*, Phys. Lett. B 447, 127 (1999).

[7] S. Fukuda *et al.*, Phys. Lett. B 539, 179 (2002).

[8] Q. R. Ahmad *et al.*, Phys. Rev. Lett. 87, 071301 (2001); Q. R. Ahmad *et al.*, Phys. Rev. Lett. 89, 011301 (2002); S. N. Ahmed *et al.*, Phys. Rev. Lett. 92, 181301 (2004).

[9] K. S. Hirata *et al.*, Phys. Lett. B 280, 146 (1992); Y. Fukuda *et al.*, Phys. Lett. B 335, 237 (1994).

[10] Y. Fukuda *et al.*, Phys. Rev. Lett. 81, 1562 (1998).

[11] W. W. M. Allison *et al.*, Phys. Lett. B 449, 137 (1999).

[12] M. Ambrosio *et al.*, Phys. Lett. B 517, 59 (2001).

[13] M. H. Ahn *et al.*, Phys. Rev. Lett. 90, 041801 (2003).

[14] D. G. Michael *et al.*, Phys. Rev. Lett. 97, 191801 (2006).

[15] K. Eguchi *et al.*, Phys. Rev. Lett. 90, 021802 (2003); T. Araki *et al.*, Phys. Rev. Lett. 94, 081801 (2005).

[16] M. Sorel, J. M. Conrad, and M. H. Shaevitz, Phys. Rev. D 70, 073004 (2004).

[17] J. A. Harvey, C. T. Hill, and R. J. Hill, arXiv:0708.1281 (2007)

[18] T. Schwetz, hep-ph/0606060 (2006).

[19] G. Barenboim *et al.*, hep-ph/0212116 (2003).

[20] G. Karagiorgi *et al.*, hep-ph/0609177 (2007).

[21] M. Maltoni, and T. Schwetz, arXiv:0705.0107 (2007).

[22] Y. Declais *et al.*, Nucl. Phys. B434, 503 (1995).

[23] A. A. Aguilar-Arevalo *et al.*, Phys. Rev. Lett. 98, 231801 (2007).

[24] J. R. Sanford and C. L. Wang, Brookhaven National Laboratory, AGS internal reports 11299 and 11479 (1967) (unpublished).

[25] M. G. Catanesi *et al.* [HARP Collaboration], arXiv:hep-ex/0702024; T. Abbott *et al.*, Phys. Rev. D45, 3906 (1992); J. V. Allaby *et al.*, CERN 70-12 (1970); D. Dekkers *et al.*, Phys. Rev. 137, B962 (1965); G. J. Marmer *et al.*, Phys. Rev. 179, 1294 (1969); T. Eichten *et al.*, Nucl. Phys. B44, 333 (1972); Aleshin *et al.*, ITEP-77-80 (1977); Vorontsov *et al.*, ITEP-88-11 (1988).

[26] A. A. Aguilar-Arevalo *et al.*, "Addendum to the MiniBooNE Run Plan: MiniBooNE Physics in 2006", submitted to the Fermilab PAC in November 2004. Available from `http://www-boone.fnal.gov/publications/`

[27] A. A. Aguilar-Arevalo *et al.*, "Addendum to the MiniBooNE Run Plan: Continued Anti-Neutrino Running in 2007", submitted to the Fermilab PAC in October 2006. Available from `http://www-boone.fnal.gov/publications/`

A Cross-Section Measurements

Increasing the anti-neutrino sample from 2.33×10^{20} POT to 5.00×10^{20} POT will clearly benefit the anti-neutrino cross-section measurements that MiniBooNE is making, since the extra statistics will shrink error bars. That having been said, the benefit is not expected to be great. Many of these measurements already have enough statistics with 2.33×10^{20} POT that they are becoming systematics limited. An exception is the wrong-sign measurement in energy bins. This analysis, described in more detail

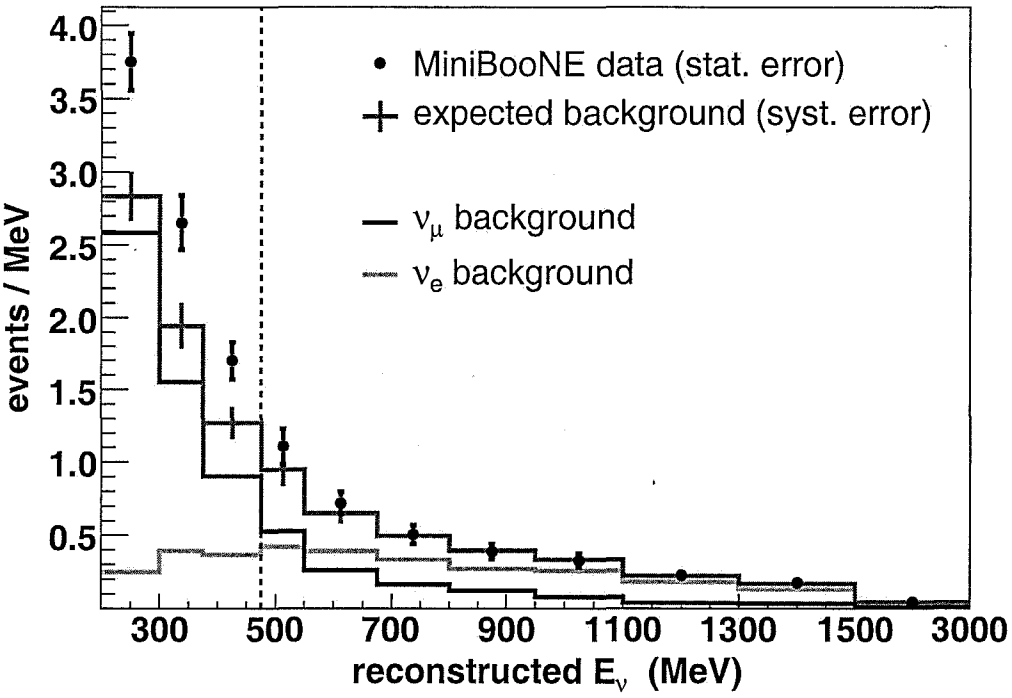

Figure 5: *This plot is identical to the upper plot of Fig. 1, but with an extra bin added at low energy from 200 to 300 MeV. See caption of Fig. 1 for details.*

in [26, 27], involves measuring the angular distribution of the muon in anti-neutrino mode CCQE interactions in bins of neutrino energy in order to extract the wrong sign (ν_μ) flux as a function of energy. Increasing the anti-neutrino mode POT would enable this analysis to bin the neutrino spectrum more finely. In addition the $\bar{\nu}_\mu$ NCπ^0 cross-section will benefit from more statistics as it has a relatively small cross-section.

B The Low Energy Excess

It was noted in Sec. 2 that MiniBooNE found an excess of ν_e candidates between 300 and 475 MeV in its ν_e appearance search. Since that time the collaboration has looked lower in energy, down to 200 MeV, and found the excess persists. This is shown in Fig. 5. (At the present time MiniBooNE is not fully confident in the systematic errors below 200 MeV and so is not willing to lower the threshold still further).

Table 3 breaks down the Monte Carlo estimated backgrounds for the three energy regions 200-300 MeV, 300-475 MeV, and 475-1250 MeV for the 5.58×10^{20} POT of the neutrino mode result (where the data numbers are also listed) and for 5.0×10^{20} POT in anti-neutrino mode. This table shows a neutrino mode excess of $91 \pm 25 \pm 19$ ν_e candidate events between 200 and 300 MeV and $95 \pm 21 \pm 19$ between 300 and 475 MeV. The two neutrino oscillation analysis region above 475 MeV shows no significant excess (hence MiniBooNE's ability to rule out two neutrino oscillations as the source of the LSND result). At this time it is not known whether the excess is due to a

		Reconstructed E_ν [MeV]		
		200-300	300-475	475-1250
5.58×10^{20} POT ν mode	Excess $\pm$(sys) $\pm$(stat)	$91 \pm 25 \pm 19$	$95 \pm 21 \pm 19$	22±35±19
	Data $\pm$(stat)	375±19	369±19	380±19
	Background $\pm$(sys)	284±25	274±21	358±35
	ν_e Intrinsic	26	67	229
	ν_μ MisID	258	207	129
	NC π^0	115	76	62
	NC $\Delta \rightarrow N\gamma$	20	51	20
	Dirt	99	50	17
	other	24	30	30
5.00×10^{20} POT $\bar{\nu}$ mode	Excess	—	—	—
	Data	—	—	—
	Background $\pm$(est. sys)	112±10	90±7	113±11
	ν_e or $\bar{\nu}_e$ Intrinsic	11	24	80
	ν_μ or $\bar{\nu}_\mu$ MisID	101	66	33
	NC π^0	42	21	15
	NC $\Delta \rightarrow N\gamma$	8	13	4
	Dirt(est. from ν mode)	45	22	7
	other	6	10	7

Table 3: *A breakdown of the backgrounds to the $\nu_e(\bar{\nu}_e)$ appearance search in three reconstructed neutrino energy bins. The top block shows the data and Monte Carlo prediction for the backgrounds for the* 5.58×10^{20} *POT published in neutrino mode. The bottom block shows the Monte Carlo background predictions (no data) for the* 5.0×10^{20} *POT being requested in anti-neutrino mode. The $\bar{\nu}$ mode dirt background has been estimated by scaling down the ν mode dirt assuming it comes from NCπ^0 interactions. Also, the $\bar{\nu}$ total systematic error on the background estimate is obtained by just scaling the ν mode systematic error. These are both expected to be tolerable approximations.*

new type of background, mis-estimated backgrounds, mis-modeled detector effects, or some beyond Standard Model physics and the collaboration is working hard to understand this. The question arises whether the anti-neutrino mode sample can help in this effort and whether 5.0×10^{20} POT in this mode provides significantly more information than 2.33×10^{20} POT. If one simply scales the neutrino mode excess down by the ratio of anti-neutrino mode to neutrino mode backgrounds one would predict an anti-neutrino mode excess of 27±6.6(sys)±10.4(stat) for 2.33×10^{20} POT and 67±16.7(sys)±16.4(stat) for 5.0×10^{20} POT (these numbers conservatively assume the systematic error is fully correlated between the two low energy bins). Thus the extra anti-neutrino mode running would turn a 2σ excess into a 3σ one.

The big question with the low energy excess is whether the extra events are electrons from a ν_e charged current process, in which case there's a strong indication of new physics creating these extra ν_es; or from gammas from ν_μ neutral current

		True Neutrino Energy [MeV]		
		200-300	300-475	475-1250
ν mode	ν_μ flux [MB^{-1} POT^{-1}]	4.076×10^{-3}	8.512×10^{-3}	3.464×10^{-2}
	$\bar{\nu}_\mu$ flux [(ν mode ν_μ flux)$^{-1}$]	0.0867	0.0587	0.0311
	ν_e flux [(ν mode ν_μ flux)$^{-1}$]	0.00609	0.00518	0.00393
	$\bar{\nu}_e$ flux [(ν mode ν_μ flux)$^{-1}$]	0.000587	0.000469	0.000363
$\bar{\nu}$ mode	ν_μ flux [(ν mode ν_μ flux)$^{-1}$]	0.125	0.0879	0.0670
	$\bar{\nu}_\mu$ flux [(ν mode ν_μ flux)$^{-1}$]	0.807	0.728	0.514
	ν_e flux [(ν mode ν_μ flux)$^{-1}$]	0.00131	0.00110	0.000747
	$\bar{\nu}_e$ flux [(ν mode ν_μ flux)$^{-1}$]	0.00420	0.00308	0.00167

Table 4: *The fluxes of the four neutrino types ($\nu_\mu, \bar{\nu}_\mu, \nu_e, \bar{\nu}_e$) in neutrino mode and in anti-neutrino mode. The fluxes are given in each of three neutrino energy bins - 200 to 300 MeV, 300 to 475 MeV, and 475 to 1250 MeV. The ν_μ flux in neutrino mode is given first in units of neutrinos crossing the MiniBooNE detector (radius 610.6cm) per proton on target. Subsequent fluxes are given in units of the neutrino mode ν_μ flux.*

processes, which would indicate mis-estimated backgrounds. The ratio of neutrino to anti-neutrino cross-sections for charged current processes in this energy range is about 3.0; the ratio for neutral current processes leading to the production of a Δ resonance is about 1.7; and the ratio for several other neutral current processes (e.g. coherent π^0 production or the recently suggested neutral current anomaly mediated photon production [17]) is about 1.0. In principle one could compare the low energy ν_e candidate excess in neutrino mode with a low energy $\bar{\nu}_e$ candidate excess in anti-neutrino mode, and then, assuming the two excesses have the same cause, use these different factors to infer whether the excesses are due to a charged current process or one or other neutral current process. The question is whether the limited statistics make the excesses in the different scenarios significantly different.

One can use the information in Table 3 together with the details of the neutrino fluxes in each mode given in Table 4 to predict anti-neutrino mode low energy excesses under each of three scenarios: 1) the excesses are due to ν_e charged current events, 2) the excesses come from mis-estimating the rate of neutral current Δ production, and 3) the excesses come from other neutral current processes whose cross-section is the same for neutrino and anti-neutrino. These three scenarios are not intented to exhaust the list of possibilities, just to provide a sampling of the range of anti-neutrino excess that might be inferred from the neutrino mode excess. The results of the calculation are shown in Table 5. Noticeably different anti-neutrino mode excesses result from the three scenarios, but the uncertainties are also large. If one considers a ratio of the excesses in neutrino and anti-neutrino mode the systematic error will be reduced as much of it is in common between the two modes. The statistical errors from the two modes will not cancel and must be combined in quadrature. Even if one sets the systematic error to zero, however, the uncertainty on the excess ratio is too large to enable a measurement of an anti-neutrino mode excess to distinguish between the three scenarios. That being said, it is always possible the anti-neutrino

		Reconstructed E_ν [MeV]	
		200-300	300-475
5.58×10^{20} POT ν mode	data excess	$91 \pm 25 \pm 19$	$95 \pm 21 \pm 19$
5.0×10^{20} POT $\bar{\nu}$ mode	ν_e CC excess	32 ± 12(stat)	28 ± 11(stat)
	ν_μ NC Δ excess	30 ± 12(stat)	31 ± 11(stat)
	other ν_μ NC excess	47 ± 13(stat)	50 ± 12(stat)

Table 5: *The first row of the table gives the measured excesses of ν_e candidates in the 200-300 and 300-475 MeV bins of the neutrino mode ν_e appearance result. The next three rows give the excesses that would result from 5.0×10^{20} POT in anti-neutrino mode under three scenarios: 1) the excesses are due to ν_e charged current events, 2) the excesses come from mis-estimating the rate of neutral current Δ production, and 3) the excesses come from other neutral current processes whose cross-section does not change in going from neutrino to anti-neutrino. The numbers in the first row are given with systematic errors first followed by statistical. All other numbers are given with just statistical errors.*

mode run may reveal an important clue to the origin of the low energy excess in a way not predicted. Perhaps there will be no excess in anti-neutrino mode or an excess even larger than that seen in the neutrino mode running.

C Oscillation Theory

Confirmation of the LSND signal in anti-neutrino mode would indicate new physics. Assuming CPT conservation, the Standard Model with three light neutrinos predicts two independent Δm^2 describing flavor transitions. Before the MiniBooNE oscillation result, the experimental situation regarding neutrino oscillations indicated three distinct mass regions at the solar, atmospheric, and LSND scales [18]. Under the assumption of CPT and CP conservation, the recent MiniBooNE oscillation analysis from neutrino mode data has ruled out a simple two neutrino oscillation interpretation of the LSND result. However, should there be any CPT or CP violation in the neutrino sector, the LSND signal would not have been fully tested, since oscillation probabilities may be different for neutrinos and anti-neutrinos. In that case, Karmen and Bugey, which are the only experiments performed in anti-neutrino mode, rule out only a portion of the LSND phase space as shown in Figure 2.

There are several models that predict CPT violation in the neutrino sector [19]. In these models neutrinos and anti-neutrinos have different Δm^2 splittings, resulting in differences between neutrino and anti-neutrino oscillation probabilities. If CPT were to be violated, then there is still the possibility of oscillations in anti-neutrino mode, which is the mode in which LSND ran. Thus, for MiniBooNE to completely rule out LSND, sufficient statistics in anti-neutrinos need to be collected. With 5×10^{20} POT in anti-neutrinos, a $\bar{\nu}_e$ appearance measurement of similar sensitivity to the MiniBooNE neutrino result can be achieved.

An interesting idea that produces differences between neutrino and anti-neutrino

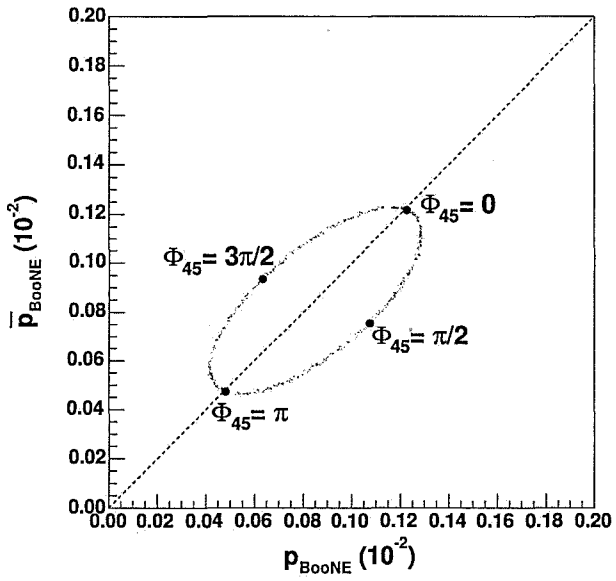

Figure 6: *Expected oscillation probabilities at MiniBooNE in neutrino and anti-neutrino running modes, for CP-violating (3+2) models [20]. Here, the neutrino masses and mixing are fixed to their best fit values from all short baseline data fits (except MiniBooNE), and CP-violating phase ϕ_{45} is allowed to vary.*

oscillation probabilities, and is more subtle than full CPT violation, is the possibility of CP violation in models with two or more sterile neutrinos. These are known as (3+2), or more generally (3+n) models [16][20].

If more than one Δm^2 contribute to the oscillations, MiniBooNE can be sensitive to a CP-violating (CPV) phase in the mixing matrix. Only appearance measurements are sensitive to such a CPV effect. This is the motivation for CPV searches at NOνA and T2K, where only the three active neutrinos are generally assumed. In the case of LSND-like oscillations, additional CPV phases may affect the CPV searches both at long and short neutrino oscillation baselines. For the case of (3+2) models [20], CPV phases can affect neutrino oscillations in short-baseline experiments, where the oscillation probability is given by:

$$P(\overset{(-)}{\nu}_\mu \to \overset{(-)}{\nu}_e) = 4|U_{e4}|^2|U_{\mu 4}|^2 \sin^2 x_{41} + 4|U_{e5}|^2|U_{\mu 5}|^2 \sin^2 x_{51} + 8|U_{e4}||U_{\mu 4}||U_{e5}||U_{\mu 5}| \sin x_{41} \sin x_{51} \cos(x_{54} \mp \phi_{45}) \quad (1)$$

where

$$x_{ji} \equiv 1.27\Delta m^2_{ji} L/E \quad \text{and} \quad \phi_{45} \equiv arg(U^*_{e4} U_{\mu 4} U_{e5} U^*_{\mu 5}). \quad (2)$$

CPV affects the oscillation probability through the interference term appearing in the second line of this equation ($\phi_{45} \to -\phi_{45}$), which can lead to differences in oscillation probabilities between neutrinos and anti-neutrinos.

Within these models, expectations for MiniBooNE neutrino and anti-neutrino running can be significantly different. Figure 6 illustrates this result for a particular

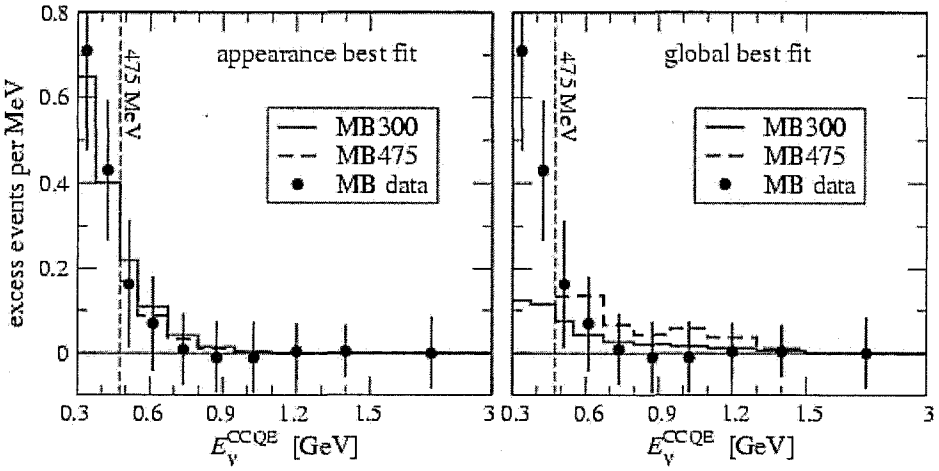

Figure 7: *MiniBooNE neutrino mode spectral data in bins of reconstructed CCQE neutrino energy. The histograms show the prediction at the best fit points in (3+2) mass schemes for SBL appearance data LSND, KARMEN, NOMAD, and MB (left), and for the global data (right). For the solid histogram the full MB energy range has been used (MB300) in the fit, whereas for the dashed histogram the two lowest energy data points have been omitted (MB475) as was done for the original MB oscillation analysis. The plots are from [21].*

sample of (3+2) models with CPV. The calculation uses the MiniBooNE neutrino and anti-neutrino mode fluxes (including ν_e and $\bar{\nu}_e$ backgrounds), thereby taking the energy dependence and wrong-sign neutrino contamination into account. The abscissa is the MiniBooNE oscillation probability that would be observed in neutrino mode and the ordinate is the oscillation probability that would be observed in anti-neutrino mode, based on the model parameters considered. One can see that CP violation may enhance or decrease the oscillation probability in anti-neutrino mode with respect to neutrino mode, depending on the value of the CPV phase. Even for small values of oscillation probability in neutrino mode, CPV can cause an enhancement (of up to 60%) in anti-neutrino mode.

An example of a CPV (3+2) model fit [21] to the recent MiniBooNE oscillation data is shown in Figure 7. Also included in the fit are the appearance measurements from KARMEN, NOMAD, and LSND (left), and all short baseline measurements, including LSND (right) [21]. Even though the low energy excess below $E_\nu^{CCQE} < 475$ MeV has not yet been substantiated, a fit was extended into this region assuming the excess events are electron neutrino candidates. As can be seen, a decent fit can be obtained in the appearance-only case. However, there is tension for global fits that include neutrino disappearance measurements. For details of the fit, see Table I in [21]. The point here is that (3+2) models with CPV have some success in fitting the short baseline data, including the MiniBooNE neutrino result and LSND anti-neutrino signal. An important consideration to note is that the (3+2) fit done here is without the MiniBooNE full error matrix. This analysis is currently being performed by MiniBooNE and will be published soon.

Based on the best-fit model parameters obtained by [21] in a global data fit with

the full MiniBooNE energy range, MiniBooNE would observe a 0.1% oscillation probability in anti-neutrino mode, $\bar{p}_{BooNE}$. Compared to the corresponding oscillation probability in neutrino mode, this would indicate an oscillation probability asymmetry of 45%. MiniBooNE's ability to discern such an asymmetry is under investigation.